AIP | Journal of Applied Physics

Microwave complex permeability of Fe3O4 nanoflake composites with and without magnetic field-induced rotational orientation

Xianguo Liu, Siu Wing Or, Chung Ming Leung, and S. L. Ho

Citation: J. Appl. Phys. **113**, 17B307 (2013); doi: 10.1063/1.4798606

View online: http://dx.doi.org/10.1063/1.4798606

View Table of Contents: http://jap.aip.org/resource/1/JAPIAU/v113/i17

Published by the AIP Publishing LLC.

JOURNAL OF APPLIED PHYSICS **113**, 17B307 (2013)

Microwave complex permeability of Fe_3O_4 nanoflake composites with and without magnetic field-induced rotational orientation

Xianguo Liu, Siu Wing Or,[a] Chung Ming Leung, and S. L. Ho
Department of Electrical Engineering, The Hong Kong Polytechnic University, Hung Hom, Kowloon, Hong Kong

(Presented 17 January 2013; received 4 November 2012; accepted 3 January 2013; published online 4 April 2013)

Magnetite (Fe_3O_4) nanoflakes with widths of 100–200 nm and thicknesses of 10–80 nm were prepared by a hydrothermal synthesis method. Fe_3O_4 nanoflake composites with and without magnetic field-induced rotational orientation of flake planes of Fe_3O_4 nanoflakes in paraffin binder were fabricated using 35 wt. % Fe_3O_4 nanoflakes. The rotationally oriented composite showed higher permeability and resonance frequency than the nonoriented one, and its value of $(\mu_0 - 1)f_r$ reached 214.8 GHz and exceeded the Snoek's limit. Considering a uniform and a random distribution of flake planes of Fe_3O_4 nanoflakes in the oriented and nonoriented composites, respectively, the complex permeability of both composites was calculated using the Landau–Lifshitz–Gilbert equation and the Bruggeman's effective medium theory in the 2–18 GHz microwave frequency range. © *2013 American Institute of Physics*. [http://dx.doi.org/10.1063/1.4798606]

An effective way to alleviate EMI pollution problems is to incorporate microwave absorbers in electromagnetic design.[1] The performance of a microwave absorber depends essentially on the magnetic and dielectric properties of the constituting materials. Advanced microwave absorbers based on core-shell-structured magnetic-dielectric nanocapsules have been a main research focus in recent years.[2–5] However, the general decrease in complex permeability with increasing microwave frequency in microwave absorbers has offered great challenges to further development and applications. To improve the microwave complex permeability, shape anisotropy in magnetic nanoparticle cores should be enhanced.[6] Flake-shaped Fe-based compound microparticles have been shown to be effective in improving complex permeability at microwave frequencies owing to their unusually high saturation magnetization and planar anisotropy.[7] This suggests that flake-shaped magnetite (Fe_3O_4) nanoparticles are suitable candidates for improving microwave complex permeability.

In this paper, we prepare flake-shaped Fe_3O_4 nanoparticles (i.e., Fe_3O_4 nanoflakes) and fabricate Fe_3O_4 nanoflake composites with and without magnetic field-induced rotational orientation of flake planes of Fe_3O_4 nanoflakes in a paraffin binder. The complex permeability of the rotationally oriented and nonoriented composites is evaluated experimentally and theoretically in the 2–18 GHz microwave frequency range. The theoretical calculation is performed on the basis of the Landau–Lifshitz–Gilbert equation and the Bruggeman's effective medium theory and is applied to explain the observed variation in complex permeability of both composites.

In a typical preparation procedure, ferrous chloride dehydrate ($FeCl_2{\cdot}2H_2O$) of 3.26 g, sodium dodecylbenzenesulfonate ($C_{18}H_{29}NaO_3S$) of 0.232 g, and sodium hydroxide (NaOH) of 1.6 g were dissolved in distilled water of 40 ml, and the solution was constantly stirred at room temperature for 20 min. The resulting blue solution was transferred into a teflon-lined stainless steel autoclave of volume 50 ml, and the autoclave was sealed and heated at 100 °C for 15 h before being cooled to room temperature naturally. The products obtained after the hydrothermal treatment were centrifuged, washed, and dried. The crystal phase of the products was identified with a Rigaku D/max 2500pc X-ray diffractometer (XRD). The morphology of the products was investigated using a Carl Zeiss Supra 35 field emission scanning electron microscope (FESEM).

Paraffin-bonded Fe_3O_4 nanoflake composites with and without magnetic field-induced rotational orientation of flake planes of Fe_3O_4 nanoflakes in a paraffin binder were fabricated using 35 wt. % Fe_3O_4 nanoflakes. For ease of description, the composites fabricated with and without magnetic field-induced rotational orientation are denoted as the rotationally "oriented" and "nonoriented" composites, respectively. The magnetic hysteresis (M–H) loop of both composites was measured using a vibrating sample magnetometer (VSM) (Lakeshore 7304). Their complex permeability values [i.e., the real (μ') and imaginary (μ'') parts of complex permeability (μ)] were determined in the 2–18 GHz range by evaluating the scattering parameters S_{11} and S_{21} using a network analyzer (Agilent 8722ES) operating in coaxial mode.

To facilitate the calculation of the complex permeability spectrum of both composites, the Landau–Lifshitz–Gilbert equation, which is derived from the precession of magnetic moments, can be described as[7]

$$\frac{dM}{dt} = -\gamma M \times H + \frac{\alpha}{M_s} M \times \frac{dM}{dt}, \tag{1}$$

where M is the magnetization, H is the effective magnetic field including the applied magnetic field, equivalent anisotropic field, demagnetization field, etc., γ (=2.8 GHz/kOe) is the gyromagnetic ratio, α is the damping coefficient, and M_S

---

[a] Author to whom correspondence should be addressed. Electronic mail: eeswor@polyu.edu.hk.

0021-8979/2013/113(17)/17B307/3/$30.00

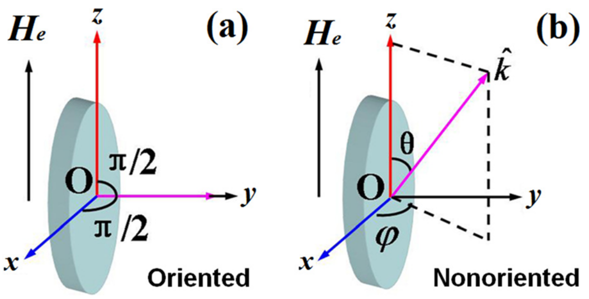

FIG. 1. Coordinate system for a single nanoflake (a) with and (b) without rotational orientation in a magnetic field.

is the saturation magnetization. The manners acting between an external microwave magnetic field and an intrinsic static magnetic field for a single nanoflake can be described by Fig. 1. H_e is the effective in-plane anisotropy field in a single nanoflake. The incident microwave has a wave vector **k**, which forms a polar angle θ with the z-axis and an azimuth angle φ in the x-y plane. Two cases are considered in our calculation: the first one is the presence of a uniform distribution of flake planes of nanoflakes (i.e., our oriented composite) [Fig. 1(a)] and the second one is the presence of a random distribution of flake planes of nanoflakes (i.e., our nonoriented composite) [Fig. 1(b)]. According to the previous report,[7] the following steps are included in our calculation: (i) calculation of the intrinsic permeability of a single nanoflake with the angles θ and φ in the rectangular coordinate system; (ii) calculation of the average permeability of numerous nanoflakes with a uniform and a random distribution of their flake planes; and (iii) calculation of the complex permeability of the composites with and without rotational orientation using the Bruggeman's effective medium theory.[7] In the rectangular coordinate system as shown in Fig. 1, H and M are expressed as

$$H = (h_x, -4\pi m_y + h_y, H_e + h_z) \tag{2a}$$

and

$$M = (m_x, m_y, M_0 + m_z), \tag{2b}$$

where M_0 is the spontaneous magnetization having a value approximately equal to M_S. By substituting Eqs. (2a) and (2b) into Eq. (1), combining them with Maxwell's equation, and considering the boundary conditions $|h| \ll |H_e|$ and $|m| \ll |M_0|$, the permeability tensor is given as[8]

$$\mu = \frac{1}{\varepsilon}\left(\frac{\delta}{j\omega}\right)^2 \begin{pmatrix} 1-\sin^2\theta\cos^2\theta & -\sin^2\theta\sin\phi\cos\phi & -\sin\theta\cos\theta\cos\phi \\ -\sin^2\theta\sin\phi\cos\phi & 1-\sin^2\theta\cos^2\phi & -\sin\theta\cos\theta\sin\phi \\ -\sin\theta\cos\theta\cos\phi & -\sin\theta\cos\theta\sin\phi & 1-\cos^2\theta \end{pmatrix}, \tag{3a}$$

$$\delta = j\omega(\mu_0\varepsilon)^{1/2}\left\{\frac{(\mu^2-\mu-\kappa^2)\sin^2\theta + 2\mu \pm [(\mu^2-\mu-\kappa^2)^2\sin^4\theta + 4\kappa^2\cos^2\theta]^{1/2}}{2[(\mu-1)\sin^2\theta+1]}\right\}^{1/2}, \tag{3b}$$

$$\mu = 1 + \frac{(\omega_0 + i\omega\alpha)\omega_m}{(\omega_0 + i\omega\alpha) - \omega^2}, \tag{3c}$$

$$\kappa = \frac{-\omega\omega_m}{(\omega_0 + i\omega\alpha)^2 - \omega^2}, \tag{3d}$$

where $\omega_0 = \gamma H_e$ and $\omega_m = \gamma 4\pi M_S$. It is noted that $\theta = \varphi = \pi/2$ is used in the case of uniform distribution of flake planes of nanoflakes (i.e., our oriented composite) [Fig. 1(a)], while randomly generated θ and φ values are employed for the case of random distribution of flake planes of nanoflakes (i.e., our nonoriented composite) [Fig. 1(b)].

For composites involving the dispersion of magnetic nanoflakes in a nonmagnetic binder, μ can be calculated by the Bruggeman's effective medium theory and the equation is described as[9]

$$p\frac{\mu_i - \mu}{\mu_i + 2\mu} + (1-p)\frac{\mu_m - \mu}{\mu_m + 2\mu} = 0, \tag{4}$$

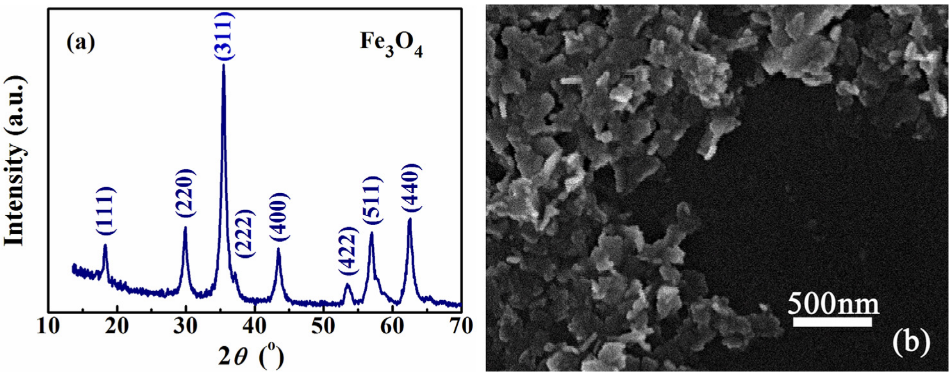

FIG. 2. Typical (a) XRD pattern and (b) SEM picture of Fe_3O_4 nanoflakes.

where p is the volume fraction of magnetic nanoflakes in the composites, μ_i is the intrinsic permeability of magnetic nanoflakes, and μ_m is the permeability of nonmagnetic binder (=1 for paraffin in this work). According to the Snoek's limit, the static relative permeability (μ_0) and the resonance frequency (f_r) have the following relationship:

$$(\mu_0 - 1)f_r = \frac{2}{3}\gamma 4\pi M_S. \tag{5}$$

While $(\mu_0 - 1)f_r$ is quantitatively greater than $\frac{2}{3}\gamma 4\pi M_S$ for bianisotropy,[6] nanoflakes with high aspect ratios have smaller in-plane anisotropy and larger out-plane anisotropy. This makes a significant contribution to achieving a bianisotropy picture and exceeding the Snoek's limit. Hence, the method of rotational orientation can effectively orient the flake planes of nanoflakes to a desired direction, thereby enhancing the effect of bianisotropy.

Figure 2(a) shows a typical XRD pattern of the as-prepared nanoparticle products. With the reflection peaks in the XRD pattern the main phase of the nanoparticle products is indexed to Fe_3O_4. Figure 2(b) illustrates a typical SEM picture of the as-prepared Fe_3O_4 nanoparticles. The Fe_3O_4 nanoparticles are in the shape of a flake with width varying from 100 to 200 nm and thickness ranging from 10 to 80 nm. These give an average width-to-thickness aspect ratio of 3:1 so that visible shape anisotropy can lead to the formation of easy magnetization planes (i.e., flake planes of the Fe_3O_4 nanoflakes).

Figure 3 plots the measured magnetic hysteresis (M–H) loop of the rotationally oriented and nonoriented Fe_3O_4 nanoflake composites. The oriented composite can be magnetized more easily compared to its nonoriented counterpart. This suggests the presence of the rotational orientation effect in the oriented composite.[7] Nonetheless, M_S of both composites is found to be ~57.5 emu/g.

Figure 4 shows the measured (symbols) and calculated (lines) complex permeabilities (μ) of the rotationally oriented and nonoriented Fe_3O_4 nanoflake composites in the 2–18 GHz range. The measured and calculated μ of both composites agree with each other. It is seen that μ' and μ'' are both higher in the oriented composite than in the nonoriented composite. In particular, the measured μ' at 2 GHz is 1.63 for the oriented composite but is only 1.25 for the nonoriented composite. The measured f_r of the oriented composite is 5.4 GHz, which is also higher than the nonoriented composite of 2.6 GHz. From the calculated results, H_e and α are found to be 500 Oe and 0.5, respectively. The calculated μ of the oriented composite increases markedly as an average factor of 1.4 in comparison with the nonoriented composite due to the effect of rotational orientation. The calculated $(\mu_0 - 1)f_r$ is 214.8 and 64.6 GHz for the oriented and nonoriented composites, respectively. These values are greater than $\frac{2}{3}\gamma 4\pi M_s$ of 27.8 GHz, indicating the presence of a bianisotropy picture and the excess of the Snoek's limit in the composites. Consequently, the coherence of the measured and calculated results proves the validity of the rotational orientation method for improving the microwave magnetic properties of nanoflake-based composites.

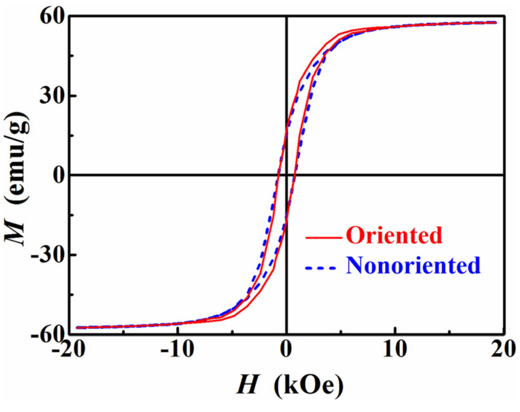

FIG. 3. Measured magnetic hysteresis (M–H) loop of rotationally oriented and nonoriented Fe_3O_4 nanoflake composites.

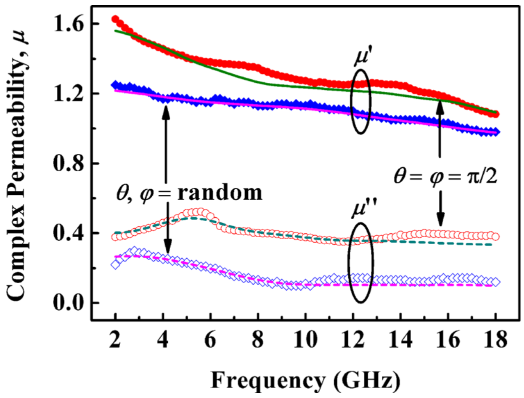

FIG. 4. Measured (symbols) and calculated (lines) complex permeabilities (μ) of rotationally oriented and nonoriented Fe_3O_4 nanoflake composites in the 2–18 GHz range.

We have prepared Fe_3O_4 nanoflakes and Fe_3O_4 nanoflake composites with and without magnetic field-induced rotational orientation. We have also established a theoretical calculation for the microwave complex permeability of the composites based on the Landau–Lifshitz–Gilbert equation and the Bruggeman's effective medium theory and applied it to explain the variation in complex permeability of the composites with and without magnetic field-induced rotational orientation. We have found that the rotationally oriented composite possesses higher permeability and resonance frequency than the nonoriented one. Moreover, its $(\mu_0 - 1)f_r$ value reaches 214.8 GHz and exceeds the Snoek's limit. The good agreement established between the measured and calculated results has confirmed the validity of applying the magnetic field-induced rotational orientation method to enhance the magnetic properties of flake-shaped nanoparticles at microwave frequencies.

This work was supported by the Research Grants Council of the HKSAR Government under Grant No. PolyU 5236/12 E and The Hong Kong Polytechnic University under Grant Nos. G-YK59, 4-ZZ7L, and G-YX3V.

[1] X. C. Tong, *Advanced Materials and Design for Electromagnetic Interference Shielding* (CRC Press, 2009).
[2] X. G. Liu *et al.*, Appl. Phys. Lett. **92**, 173117 (2008).
[3] X. G. Liu *et al.*, Carbon **47**, 470 (2009).
[4] X. G. Liu *et al.*, J. Alloys Compd. **509**, 2929 (2011).
[5] X. G. Liu *et al.*, J. Alloys Compd. **509**, 9071 (2011).
[6] D. S. Xue *et al.*, Chin. Phys. Lett. **25**, 4120 (2008).
[7] W. F. Yang *et al.*, J. Appl. Phys. **107**, 033913 (2010).
[8] L. Z. Wu *et al.*, J. Appl. Phys. **99**, 083905 (2006).
[9] D. Rousselle *et al.*, J. Appl. Phys. **74**, 475 (1993).